

# Introduction of stratospheric aerosol features in EarthCARE's aerosol classification model

Athena A. Floutsi<sup>(a)</sup>, Holger Baars<sup>(a)</sup>, Georg H. Müller<sup>(a)</sup>, Moritz Haarig<sup>(a)</sup>, Albert Ansmann<sup>(a)</sup> and Ulla Wandinger<sup>(a)</sup>

(a) Leibniz Institute for Tropospheric Research (TROPOS)  
Permoserstraße 15, 04318 Leipzig, Germany  
[floutsi@tropos.de](mailto:floutsi@tropos.de)

**Abstract:** The extension of the Hybrid End-To-End Aerosol Classification (HETEAC) model with respect to stratospheric targets is presented. The methodology follows the HETEAC approach, i.e., a suitable set of basic feature types is defined to allow for scattering calculations. The most appropriate microphysical representation is selected based on the agreement between optical properties derived from scattering calculations and ground-based lidar observations. The extended HETEAC model (2.0), considers stratospheric features such as sulfate, volcanic ash, and smoke particles and also polar stratospheric clouds (PSCs). HETEAC 2.0 ensures consistency with the CALIPSO (Cloud-Aerosol Lidar and Infrared Pathfinder Satellite Observations) approach, which is of great importance for the harmonization of long-term satellite records.

## 1. Introduction

The HETEAC model, which serves as the common baseline for the development, evaluation, and implementation of EarthCARE algorithms has been introduced recently [1]. The model's hybrid approach ensures consistency between the theoretical description of aerosol microphysics and the experimentally derived optical properties [2], while the end-to-end approach allows for a complete and uniform representation of the aerosol types in terms of microphysical, optical, and radiative properties.

HETEAC considers four aerosol components: two fine modes consisting of either weakly or strongly absorbing spherical particles and two coarse modes consisting of either spherical or non-spherical particles. The four aerosol components reflect adequately the most frequently observed aerosol types in the troposphere: pollution-related aerosol, fresh smoke, marine particles, and desert dust, respectively.

Currently, HETEAC does not consider any stratospheric aerosols and polar stratospheric clouds (PSCs). Therefore, to improve the processing in the stratosphere, e.g., with respect to target classification and smoothing strategies, the HETEAC model is being extended. HETEAC 2.0 will include all stratospheric features, i.e., aerosols and PSCs. Since PSCs are optically thin and consist of relatively small

particles in the sub-micron to few microns size range, they can be treated like aerosols in HETEAC 2.0. To avoid confusion and to be consistent with the CALIPSO terminology, we use the generic term stratospheric feature to include both aerosol and PSCs.

## 2. Methodology

The first step of the approach is the definition of a suitable set of basic feature types based on ground-based lidar observations (see Sect. 3). Since aerosol in the upper troposphere and lower stratosphere (UTLS) as well as in higher stratospheric altitudes is mostly of natural origin, all stratospheric aerosol types considered are natural aerosol. In particular, there are three major aerosol types, sulfates, volcanic ash, and smoke. For PSCs, we follow the common classification into PSCs of type Ia, Ib, and II. Then, all feature types need to be described in terms of microphysical properties (i.e., size, shape, and refractive index) to allow for scattering calculations. The most appropriate microphysical representation is selected based on the agreement between optical properties derived from scattering calculations and ground-based lidar observations (e.g., lidar ratio, particle linear depolarization ratio). The final step is the creation of a Look-Up Table (LUT) of the related optical and radiative properties (i.e., asymmetry parameter, single-scattering albedo)

for each feature type and also for certain mixtures.

**Table 1. Overview of the different stratospheric feature types, along with the references for the measurements that were used for the creation of the experimental basis.**

Aerosol type	Reference(s)
Volcanic ash	[3, 4]
Smoke	[5]
PSC-Ia	[6]
PSC-Ib	[6, 7]
PSC-II	[6]

### 3. Experimental basis

Figure 1 shows the currently available collection of lidar-derived intensive optical properties at the EarthCARE wavelength of 355 nm. The collection is mostly based on ground-based lidar measurements available in the literature (Table 1) as well as from measurements conducted with TROPOS-built lidar systems. As can be seen, stratospheric measurements at 355 nm are very rare, since most observations are made at 532 nm.

Measurements conducted with the PollyXT Arielle system of the OCEANET-Atmosphere facility at Neumayer III Station, Antarctica, in the southern hemispheric winter of 2023 are an important addition to the experimental basis. In Fig. 1, they have been marked separately, even though they fall into the PSC II category, as the analysis is not yet complete. With the completion of the analysis more data points are expected, also for the other PSC categories.

### 4. Feature Types

To adequately describe the aforementioned feature types, new pure particle components are introduced in HETEAC for the stratosphere. A total of seven feature types are considered in HETEAC 2.0. These feature types are presented in Fig. 2 and briefly introduced in the following sections.

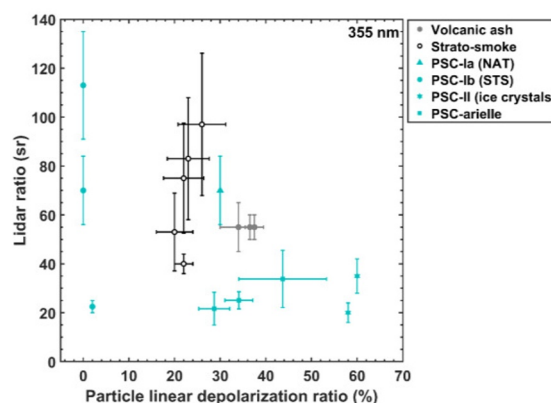


Figure 1. Intensive optical properties of different stratospheric feature types at 355 nm.

#### 4.1. Sulfate aerosol

For classification purposes, all sulfate aerosol is assumed to consist of 75 %  $H_2SO_4$  and 25 %  $H_2O$ . The particles are also assumed to be spherical (liquid droplets), thus, causing no depolarization. The imaginary part of the refractive index is set to zero since absorption for sulfates is very low for visible and near-infrared radiation [8]. On the other hand, the real part of the refractive index is varying depending on the sulfuric acid content, which in turn is dependent on height, temperature, and humidity. The real part of the refractive index is currently set to 1.45 (at 355 nm), which is found to be a realistic assumption [9,10]. Given the aforementioned characteristics, the component attributed to sulfate aerosol is a spherical, non-absorbing fine mode. Due to the differences in the origin, the sulfate category is split further into two components, one resembling the background conditions and one to capture the presence of sulfate aerosol due to a volcanic event. Both sub-components can be described with a log-normal size distribution of spherical particles, however, the distribution for the background sulfate aerosol is mono-modal, while it is bi-modal for the volcanic sulfate aerosol [9].

#### 4.2. Volcanic Ash

Volcanic ash particles are challenging to model not only due to their irregular shape, but also due to their refractive index, which is unique to each eruption because of the different minerals involved. A way to overcome this challenge would be to use an average refractive index of several samples taken during different eruptions, which at the moment is not available at 355 nm. Volcanic ash can be represented by

non-spherical, moderately absorbing coarse-mode particles. Studies [11] have shown similarities between the size distributions of volcanic ash and dust and, therefore, our starting point for the parameterizing of volcanic ash in HETEAC 2.0 is the “coarse mode, non-spherical” HETEAC component that resembles dust.

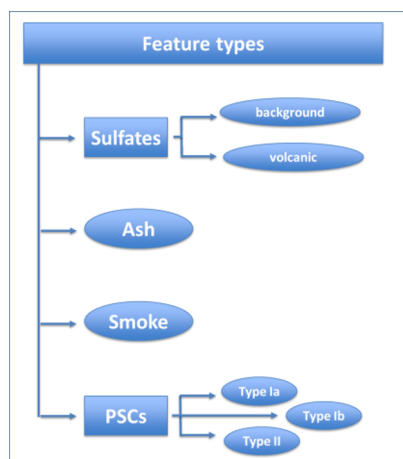


Figure 2. The seven stratospheric feature types of HETEAC 2.0 (in the elliptical shapes).

### 4.3. Smoke

The optical properties of smoke in the stratosphere have been studied intensively by means of ground-based lidar systems [e.g., 12, 13]. In contrast to smoke in the troposphere, which contains mainly spherical particles, stratospheric smoke often consists of non-spherical particles, yielding high depolarization ratios (at both 355 and 532 nm). This feature is therefore represented by a component consisting of non-spherical, absorbing, fine-mode particles.

### 4.4. PSCs

PSCs occur in the polar vortex at very low temperatures. Therefore, the HETEAC 2.0 components that resemble PSCs are allowed only in the stratosphere above the poles and during winter. There are three distinctive PSC types, namely Type Ia, which consists of tiny nitric acid trihydrate (NAT) crystals, Type Ib, which is made up of droplets of a supercooled ternary solution (STS), and Type II, which contains small ice crystals. Types Ia and Ib start forming at temperatures around 195 K, while Type II occurs at temperatures below approximately 188 K. These thermodynamic requirements, along with the aforementioned spatiotemporal requirements, for the PSC

formation are a great advantage for classification purposes. In particular, for HETEAC 2.0 they are utilized in a form of pre-classification tree (see Fig. 3) for the identified stratospheric feature. This approach also ensures consistency with the CALIPSO approach (version 4.5, [14]).

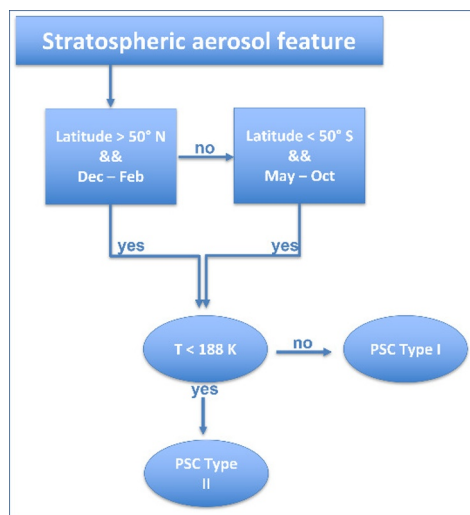


Figure 3. Decision tree that takes into account thermodynamic and spatiotemporal information and allows for a pre-classification (Type I or II) of the PSCs.

#### 4.4.1. PSC Type Ia (NAT)

Type Ia PSCs are composed of non-spherical, fine-mode particles that are also non-absorbing. Following [15] we assume a fixed real part of the refractive index equal to 1.50. The imaginary part is assumed to be 0.0 (in practice, it is set to 1.00E-10).

#### 4.4.2. PSC Type Ib (STS)

STS or Type Ib PSCs can be represented by spherical, non-absorbing, fine-mode particles. As for Type Ia, we assume a fixed real part of the refractive index equal to 1.43 and an imaginary part equal to 0.0 (in practice, it is set to 1.00E-10; [15]).

#### 4.4.3. PSC Type II (ice)

Type II PSCs can be represented by non-spherical, non-absorbing, coarse-mode particles. For ice, the refractive index is set to 1.308 [15]. Similarly to NAT particles, the shape of the ice crystals can be assumed to be oblate spheroidal particles with an axis ratio of 1.2 [15].

## 5. Outlook

Calculations of the scattering properties are currently ongoing mainly using the Dubovik spheroidal model [16]. An important step towards the finalization and implementation of HETEAC 2.0 is the extension of the experimental basis. Stratospheric feature types such as sulfates and PSCs are at the moment underrepresented, since measurements at 355 nm are very rare. Once the microphysical description is finalized, HETEAC 2.0 will be implemented in a similar way as HETEAC, i.e., in the form of a LUT.

## 6. References

- [1] Wandinger, U., Floutsi, A. A., Baars, H., Haarig, M., Ansmann, A., Hünerbein, A., Docter, N., Donovan, D., van Zadelhoff, G.-J., Mason, S., and Cole, J.: HETEAC – the Hybrid End-To-End Aerosol Classification model for EarthCARE, *Atmos. Meas. Tech.*, **16**, 2485–2510, 2023.
- [2] Floutsi, A. A., Baars, H., Engelmann, R., Althausen, D., Ansmann, A., Bohlmann, S., Heese, B., Hofer, J., Kanitz, T., Haarig, M., Ohneiser, K., Radenz, M., Seifert, P., Skupin, A., Yin, Z., Abdullaev, S. F., Komppula, M., Filioglou, M., Giannakaki, E., Stachlewska, I. S., Janicka, L., Bortoli, D., Marinou, E., Amiridis, V., Gialitaki, A., Mamouri, R.-E., Barja, B., and Wandinger, U.: DeLiAn – a growing collection of depolarization ratio, lidar ratio and Ångström exponent for different aerosol types and mixtures from ground-based lidar observations, *Atmos. Meas. Tech.*, **16**, 2353–2379, 2023.
- [3] Groß, S., Freudenthaler, V., Wiegner, M., Gasteiger, J., Geiß, A., and Schnell, F.: Dual-wavelength linear depolarization ratio of volcanic aerosols: Lidar measurements of the Eyjafjallajökull plume over Maisach, Germany, *Atmos. Environ.*, **48**, 85–96, 2012.
- [4] Kanitz, T.: Vertical distribution of aerosols above the Atlantic Ocean, Punta Arenas (Chile), and Stellenbosch (South Africa), PhD dissertation, Technische Universität Berlin, 2012.
- [5] Ohneiser, K., Ansmann, A., Baars, H., Seifert, P., Barja, B., Jimenez, C., Radenz, M., Tisseire, A., Floutsi, A., Haarig, M., Foth, A., Chudnovsky, A., Engelmann, R., Zamorano, F., Bühl, J., and Wandinger, U.: Smoke of extreme Australian bushfires observed in the stratosphere over Punta Arenas, Chile, in January 2020: optical thickness, lidar ratios, and depolarization ratios at 355 and 532 nm, *Atmos. Chem. Phys.*, **20**, 8003–8015, 2020.
- [6] Reichardt, J., Dörnbrack, A., Reichardt, S., Yang, P., and McGee, T. J.: Mountain wave PSC dynamics and microphysics from ground-based lidar measurements and meteorological modeling, *Atmos. Chem. Phys.*, **4**, 1149–1165, 2004.
- [7] Böckmann, C., Ritter, C.: Properties of Polar Stratospheric Clouds over the European Arctic from Ground-Based Lidar. In: Sullivan, J.T., et al. *Proceedings of the 30th International Laser Radar Conference. ILRC 2022. Springer Atmospheric Sciences. Springer, Cham. 2023.*
- [8] Palmer K. F. and Williams D.: "Optical Constants of Sulfuric Acid; Application to the Clouds of Venus?," *Appl. Opt.* **14**, 208-219, 1975.
- [9] Wandinger, U., Ansmann, A., Reichardt, J., and Deshler, T.: Determination of stratospheric aerosol microphysical properties from independent extinction and backscattering measurements with a Raman lidar, *Applied Optics*, **34**, 8315–8329, 1995.
- [10] Beyer, K.D., Ravishankara, A.R. and Lovejoy, E.R.: Measurements of UV refractive indices and densities of H<sub>2</sub>SO<sub>4</sub>/H<sub>2</sub>O and H<sub>2</sub>SO<sub>4</sub>/HNO<sub>3</sub>/H<sub>2</sub>O solutions, *Journal of Geophysical Research: Atmospheres*, **101**(D9), pp.14519-14524, 1996.
- [11] Winker, D. M., Z. Liu, A. Omar, J. Tackett, and D. Fairlie: CALIOP observations of the transport of ash from the Eyjafjallajökull volcano in April 2010, *J. Geophys. Res.*, **117**, D00U15, 2012.
- [12] Ansmann, A., Baars, H., Chudnovsky, A., Mattis, I., Veselovskii, I., Haarig, M., Seifert, P., Engelmann, R., and Wandinger, U.: Extreme levels of Canadian wildfire smoke in the stratosphere over central Europe on 21-22 August 2017, *Atmos. Chem. Phys.*, **18**, 11 831–11 845, 2018.
- [13] Haarig, M., Ansmann, A., Baars, H., Jimenez, C., Veselovskii, I., Engelmann, R., and Althausen, D.: Depolarization and lidar ratios at 355, 532, and 1064 nm and microphysical properties of aged tropospheric and stratospheric Canadian wildfire smoke, *Atmos. Chem. Phys.*, **18**, 11 847–11 861, <https://doi.org/10.5194/acp-18-11847-2018>, 2018.
- [14] Tackett, J. L., Kar, J., Vaughan, M. A., Getzewich, B. J., Kim, M.-H., Vernier, J.-P., Omar, A. H., Magill, B. E., Pitts, M. C., and Winker, D. M.: The CALIPSO version 4.5 stratospheric aerosol subtyping algorithm, *Atmos. Meas. Tech.*, **16**, 745–768, 2023.
- [15] Pitts, M. C., Poole, L. R., and Thomason, L. W.: CALIPSO polar stratospheric cloud observations: second-generation detection algorithm and composition discrimination, *Atmos. Chem. Phys.*, **9**, 7577–7589, 2009.
- [16] Dubovik, O., A. Sinyuk, T. Lapyonok, B.N. Holben, M. Mishchenko, P. Yang, T.F. Eck, H. Volten, O. Muñoz, B. Veißelmann, W.J. van der Zande, J.-F. Leon, M. Sorokin, and I. Slutsker.: Application of spheroid models to account for aerosol particle non sphericity in remote sensing of desert dust. *J. Geophys. Res.*, **111**, D11208, 2006.